PHYSICAL REVIEW C VOLUME 32, NUMBER 5 NOVEMBER 1985

Kaon photoproduction operator for use in nuclear physics

R. A. Adelseck, C. Bennhold, and L. E. Wright
Physics Department, Ohio University, Athens, Ohio 45701
(Received 28 January 1985; revised manuscript received 17 June 1985)

Using diagrammatic techniques we have obtained a new operator for the process $p(\gamma,K^+)\Lambda^0$ which includes the Born terms in addition to resonances in the s and u channel near threshold. The coupling constants are obtained by a least squares fit to cross section and polarization data for photon energies from threshold through 1400 MeV. We find a number of changes from the earlier operator obtained by Thom about twenty years ago when less data were available. To aid in comparing this operator to other work, we give its multipole decomposition in the center of mass frame, and to aid in its use in nuclear physics we write out the operator in a frame fixed in the nucleus and, further, take the nonrelativistic limit of the operator as Blomqvist and Laget did for the pion photoproduction case. Finally, we discuss the validity of the nonrelativistic limit of this operator.

I. INTRODUCTION

With the advent of continuous wave electron linacs with higher energy and intensity, the reaction $p(\gamma,K^+)\Lambda^0$ has great prospects for becoming an important probe of the nuclear interior.[1,2] Both the photon and the positively charged kaon interact rather weakly with the nucleus so that the reaction can occur deep in the nucleus. For the case where the Λ^0 remains bound in the nucleus this will permit the study of deep lying hypernuclear states.

The analysis of photoproduction of kaons from nuclei is most straightforwardly carried out with a distorted wave impulse approximation whereby the incoming gamma interacts with a proton in the nucleus to produce a K^+ and a Λ^0. The Λ^0 goes into some bound state, while the K^+ exits the nucleus interacting with the remaining $A-1$ nucleons via a rather weak optical potential. The basic ingredient to such an analysis, which is similar to previous work on pion photoproduction and electroproduction,[3,4] is the kaon production operator from the free nucleon.

Thom[5] wrote a kaon photoproduction operator in 1966 using Feynman diagrams for the Born terms and partial-wave amplitudes for the resonances. Since that time more data have become available, making it necessary to reexamine Thom's results. Moreover, since the struck proton is in motion in the nucleus, one requires a frame independent kaon production operator. Therefore, resonant terms, such as the ones used by Thom,[5] are not appropriate because of their transformation properties. For this reason we derive in Sec. II the scattering amplitude by using diagrammatic techniques for the Born terms as well as for the resonant terms. This assures the relativistic invariance of the operator. In Sec. III we decompose the amplitude into its multipoles following a procedure by Berends *et al.*[6] for use in comparison with other work and for future considerations of unitarity constraints. For use in nuclear physics we take the nonrelativistic limit of the operator in Sec. IV and discuss the validity of this approximation in a system where rather large energies and momenta are present. In Sec. V we give a table of all coupling constants obtained and compare the theoretical predictions of different models with data. A collection of all data used in fitting the coupling constants is given in Tables VI and VII.

II. DERIVATION OF THE OPERATOR

Throughout the paper we use the notation and conventions of Bjorken and Drell.[7] Figures 1(a)—(e) show the Feynman diagrams for the nonresonant background or Born terms for the reaction $p(\gamma,K^+)\Lambda^0$. Using the procedure described by, e.g., Gourdin and Dufour,[8] the S-matrix elements can be written as

$$S_{fi}=\frac{1}{(2\pi)^2}\left[\frac{M_p M_\Lambda}{4E_\Lambda E_K E_p E_\gamma}\right]^{1/2} M_{fi}\delta^4(p_p+p_\gamma-p_K-p_\Lambda)\ , \tag{1}$$

where the matrix element

$$M_{fi}=\bar{u}(p_\Lambda,s_\Lambda)\sum_{j=1}^{4} A_j M_j u(p_p,s_p)\ .$$

The matrices M_i are given by

$$\begin{aligned} M_1&=-\gamma_5 \not\epsilon \not p_\gamma\ ,\\ M_2&=2\gamma_5(\epsilon\cdot p_p p_\gamma\cdot p_\Lambda-\epsilon\cdot p_\Lambda p_\gamma\cdot p_p)\ ,\\ M_3&=\gamma_5(\not\epsilon p_\gamma\cdot p_p-\not p_\gamma \epsilon\cdot p_p)\ ,\\ M_4&=\gamma_5(\not\epsilon p_\gamma\cdot p_\Lambda-\not p_\gamma \epsilon\cdot p_\Lambda)\ , \end{aligned} \tag{2}$$

where $p_\gamma=(E_\gamma,\mathbf{p}_\gamma)$, p_p, p_K, and p_Λ are the four-vectors of the photon, proton, kaon, and lambda, respectively. The amplitudes A_i are given in Table I using the following definition of the Mandelstam variables:

$$s=(p_p+p_\gamma)^2,\ \ t=(p_\gamma-p_K)^2,\ \ u=(p_p-p_K)^2\ .$$

It should be noted that the amplitudes as well as the matrices are Lorentz and gauge invariant. They are related to the cross section by the expression

TABLE I. Invariant amplitudes for the reaction $\gamma+\mathrm{p}\rightarrow\mathrm{K}^{+}+\Lambda^{0}$.

$$A_1=\frac{g_{\Lambda}e}{s-M_{\mathrm{p}}^2}(1+\kappa_{\mathrm{p}})+\frac{g_{\Lambda}e}{u-M_{\Lambda}^2}\kappa_{\Lambda}+\frac{G_{\Sigma}e}{u-M_{\Sigma}^2}+\frac{G_V}{M}\frac{(M_{\Lambda}+M_{\mathrm{p}})}{t-M_{K^*}^2}+\frac{G_T t}{M(M_{\mathrm{p}}+M_{\Lambda})}\frac{1}{t-M_{K^*}^2}+\frac{G_{\mathrm{N1}}e}{s-M_{\mathrm{N1}}^2+iM_{\mathrm{N1}}\Gamma_{\mathrm{N1}}}\left[1-i\frac{\Gamma_{\mathrm{N1}}}{2(M_{\mathrm{N1}}+M_{\mathrm{p}})}\right]$$

$$+\frac{G_{\mathrm{N4}}e}{s-M_{\mathrm{N4}}^2+iM_{\mathrm{N4}}\Gamma_{\mathrm{N4}}}\left[\frac{M_{\mathrm{N4}}-M_{\mathrm{p}}}{M_{\mathrm{N4}}+M_{\mathrm{p}}}-i\frac{\Gamma_{\mathrm{N4}}}{2(M_{\mathrm{N4}}+M_{\mathrm{p}})}\right]+\frac{1}{3(s-M_{\mathrm{N5}}^2+iM_{\mathrm{N5}}\Gamma_{\mathrm{N5}})(\sqrt{s}-M_{\mathrm{p}})M_{\mathrm{N5}}}$$

$$\times\left\{G_{\mathrm{N5}}^1\left[\frac{M_{\Lambda}^2-M_{\mathrm{K}}^2+s}{2s}(3s-2\sqrt{s}M_{\mathrm{p}}-M_{\mathrm{p}}^2)-\frac{M_{\Lambda}}{2\sqrt{s}}(3s-4\sqrt{s}M_{\mathrm{p}}+M_{\mathrm{p}}^2)+\tfrac{3}{2}(u-M_{\Lambda}^2)\right]+G_{\mathrm{N5}}^2\frac{s-M_{\mathrm{p}}^2}{2(\sqrt{s}-M_{\mathrm{p}})}\left[M_{\Lambda}-\frac{M_{\Lambda}^2-M_{\mathrm{K}}^2+s}{2\sqrt{s}}\right]\right\}$$

$$+\frac{1}{3(s-M_{\mathrm{N7}}^2+iM_{\mathrm{N7}}\Gamma_{\mathrm{N7}})(\sqrt{s}+M_{\mathrm{p}})M_{\mathrm{N7}}}\left\{G_{\mathrm{N7}}^1\left[\frac{M_{\Lambda}^2-M_{\mathrm{K}}^2+s}{2s}(3s+2\sqrt{s}M_{\mathrm{p}}-M_{\mathrm{p}}^2)+\frac{M_{\Lambda}}{2\sqrt{s}}(3s+4\sqrt{s}M_{\mathrm{p}}+M_{\mathrm{p}}^2)+\tfrac{3}{2}(u-M_{\Lambda}^2)\right]\right.$$

$$\left.+G_{\mathrm{N7}}^2\frac{s-M_{\mathrm{p}}^2}{2(\sqrt{s}+M_{\mathrm{p}})}\left[-M_{\Lambda}-\frac{M_{\Lambda}^2-M_{\mathrm{K}}^2+s}{2\sqrt{s}}\right]\right\}+\frac{G_{\mathrm{Y5}}e}{u-M_{\mathrm{Y5}}^2+iM_{\mathrm{Y5}}\Gamma_{\mathrm{Y5}}}\left[\frac{M_{\mathrm{Y5}}-M_{\Lambda}}{M_{\mathrm{Y5}}+M_{\Lambda}}-i\frac{\Gamma_{\mathrm{Y5}}}{2(M_{\mathrm{Y5}}+M_{\Lambda})}\right],$$

$$A_2=\frac{2g_{\Lambda}e}{(t-M_{\mathrm{K}}^2)(s-M_{\mathrm{p}}^2)}+\frac{G_T}{M(M_{\mathrm{p}}+M_{\Lambda})}\frac{1}{t-M_{\mathrm{K}^*}^2}+\frac{1}{3(s-M_{\mathrm{N5}}^2+iM_{\mathrm{N5}}\Gamma_{\mathrm{N5}})(\sqrt{s}-M_{\mathrm{p}})M_{\mathrm{N5}}}$$

$$\times\left[-3G_{\mathrm{N5}}^1+G_{\mathrm{N5}}^2\frac{3(\sqrt{s}+M_{\mathrm{p}})}{2(\sqrt{s}-M_{\mathrm{p}})}\right]+\frac{1}{3(s-M_{\mathrm{N7}}^2+iM_{\mathrm{N7}}\Gamma_{\mathrm{N7}})(\sqrt{s}+M_{\mathrm{p}})M_{\mathrm{N7}}}\left[-3G_{\mathrm{N7}}^1+G_{\mathrm{N7}}^2\frac{3(\sqrt{s}-M_{\mathrm{p}})}{2(\sqrt{s}+M_{\mathrm{p}})}\right],$$

$$A_3=\frac{g_{\Lambda}e}{s-M_{\mathrm{p}}^2}\frac{\kappa_{\mathrm{p}}}{M_{\mathrm{p}}}+\frac{G_{\Lambda}}{M}\frac{1}{t-M_{\mathrm{K}^*}^2}-\frac{G_T}{M(M_{\mathrm{p}}+M_{\Lambda})}\frac{M_{\Lambda}-M_{\mathrm{p}}}{t-M_{\mathrm{K}^*}^2}+\frac{2G_{\mathrm{N1}}e}{s-M_{\mathrm{N1}}^2+iM_{\mathrm{N1}}\Gamma_{\mathrm{N1}}}\frac{1}{M_{\mathrm{N1}}+M_{\mathrm{p}}}-\frac{2G_{\mathrm{N4}}e}{s-M_{\mathrm{N4}}^2+iM_{\mathrm{N4}}\Gamma_{\mathrm{N4}}}\frac{1}{M_{\mathrm{N4}}+M_{\mathrm{p}}}+\frac{1}{3(s-M_{\mathrm{N5}}^2+iM_{\mathrm{N5}}\Gamma_{\mathrm{N5}})(\sqrt{s}-M_{\mathrm{p}})M_{\mathrm{N5}}}$$

$$\times\left\{G_{\mathrm{N5}}^1\left[\frac{M_{\Lambda}}{\sqrt{s}}(3\sqrt{s}-M_{\mathrm{p}})-\frac{M_{\Lambda}^2-M_{\mathrm{K}}^2+s}{s}M_{\mathrm{p}}\right]+G_{\mathrm{N5}}^2\frac{1}{\sqrt{s}-M_{\mathrm{p}}}\left[\left[\frac{M_{\Lambda}^2-M_{\mathrm{K}}^2+s}{2\sqrt{s}}-M_{\Lambda}\right](\sqrt{s}+M_{\mathrm{p}})+\frac{3(u-M_{\Lambda}^2)}{2}\right]\right\}$$

$$+\frac{1}{3(s-M_{\mathrm{N7}}^2+iM_{\mathrm{N7}}\Gamma_{\mathrm{N7}})(\sqrt{s}+M_{\mathrm{p}})M_{\mathrm{N7}}}\left\{G_{\mathrm{N7}}^1\left[\frac{M_{\Lambda}}{\sqrt{s}}(3\sqrt{s}+M_{\mathrm{p}})-\frac{M_{\Lambda}^2-M_{\mathrm{K}}^2+s}{s}M_{\mathrm{p}}\right]-G_{\mathrm{N7}}^2\frac{1}{\sqrt{s}+M_{\mathrm{p}}}\left[\left[\frac{M_{\Lambda}^2-M_{\mathrm{K}}^2+s}{2\sqrt{s}}+M_{\Lambda}\right](\sqrt{s}-M_{\mathrm{p}})+\frac{3(u-M_{\Lambda}^2)}{2}\right]\right\},$$

$$A_4=\frac{g_{\Lambda}e}{u-M_{\Lambda}^2}\frac{\kappa_{\Lambda}}{M_{\Lambda}}+\frac{G_{\Sigma}e}{u-M_{\Sigma}^2}\frac{2}{M_{\Sigma}+M_{\Lambda}}+\frac{G_{\Lambda}}{M}\frac{1}{t-M_{\mathrm{K}^*}^2}+\frac{G_T}{M}\frac{M_{\Lambda}-M_{\mathrm{p}}}{M_{\Lambda}+M_{\mathrm{p}}}\frac{1}{t-M_{\mathrm{K}^*}^2}$$

$$+\frac{1}{(s-M_{\mathrm{N5}}^2+iM_{\mathrm{N5}}\Gamma_{\mathrm{N5}})M_{\mathrm{N5}}}\left[-G_{\mathrm{N5}}^1+G_{\mathrm{N5}}^2\frac{s-M_{\mathrm{p}}^2}{2(\sqrt{s}-M_{\mathrm{p}})^2}\right]+\frac{1}{(s-M_{\mathrm{N7}}^2+iM_{\mathrm{N7}}\Gamma_{\mathrm{N7}})M_{\mathrm{N7}}}\left[G_{\mathrm{N7}}^1-G_{\mathrm{N7}}^2\frac{s-M_{\mathrm{p}}^2}{2(\sqrt{s}+M_{\mathrm{p}})^2}\right]-\frac{2G_{\mathrm{Y5}}e}{u-M_{\mathrm{Y5}}^2+iM_{\mathrm{Y5}}\Gamma_{\mathrm{Y5}}}\frac{1}{M_{\mathrm{Y5}}+M_{\Lambda}}$$

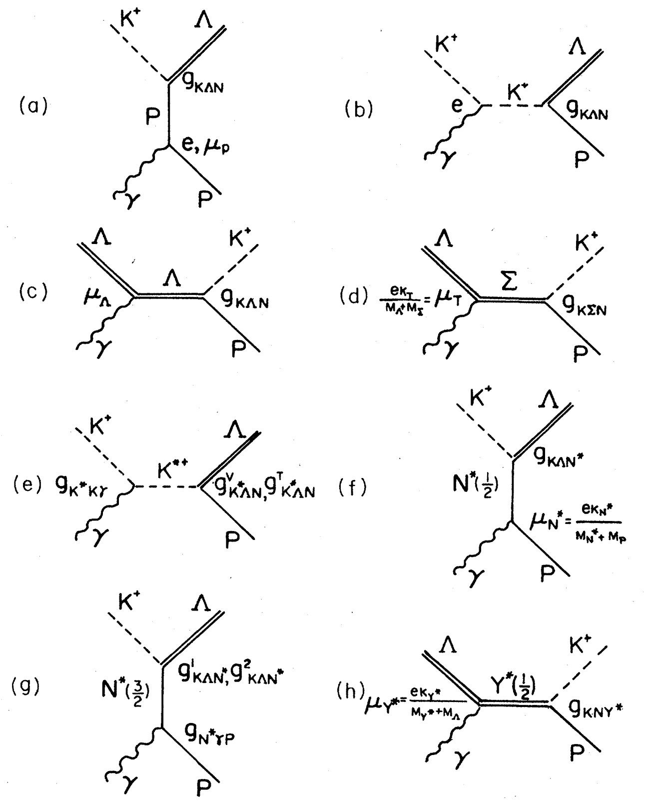

FIG. 1. Feynman diagrams for the process $\gamma+\mathrm{p}\rightarrow\mathrm{K}^{+}+\Lambda^{0}$. (a)—(e) represent the Born terms including the vector kaon exchange, (f) and (g) stand for spin $\frac{1}{2}$ and $\frac{3}{2}$ resonant terms in the s channel, and (h) represents spin $\frac{1}{2}$ resonant terms in the u channel.

$$d\sigma=(2\pi)^4\frac{M_{\mathrm{p}}M_{\Lambda}\,|M_{fi}\,|^2\delta^4(p_{\mathrm{p}}+p_{\gamma}-p_{\mathrm{K}}-p_{\Lambda})}{4E_{\Lambda}E_{\mathrm{K}}[(p_{\mathrm{p}}\cdot p_{\gamma})^2-p_{\mathrm{p}}^2p_{\gamma}^2]^{1/2}} \times\frac{d^3p_{\mathrm{K}}d^3p_{\Lambda}}{(2\pi)^3(2\pi)^3}\ . \tag{3}$$

Of the nine different coupling constants involved in the amplitudes A_i, the charge e and magnetic moment μ_{p} of the proton are well known, and the magnetic moment μ_{Λ} of the lambda has recently been determined to be $(-0.6138\pm0.0047)\,\mu_{\mathrm{N}}$.[9] The remaining six constants can be grouped into four effective constants

$$\begin{aligned} g_{\Lambda}&=g_{\mathrm{K}\Lambda\mathrm{N}}\ ,\\ G_{\Sigma}&=\kappa_T g_{\mathrm{K}\Sigma\mathrm{N}}\ ,\\ G_V&=g_{\mathrm{K}^*\mathrm{K}\gamma}g^{V}_{\mathrm{K}^*\Lambda\mathrm{N}}\ ,\\ G_T&=g_{\mathrm{K}^*\mathrm{K}\gamma}g^{T}_{\mathrm{K}^*\Lambda\mathrm{N}}\ , \end{aligned} \tag{4}$$

which can be determined by a least squares fit to cross section and polarization data (see Tables VI and VII). Using these parameters (see Table V in Sec. V), however, the obtained χ^2 is rather large indicating that this simple operator is not sufficient for the description of the photoproduction process. Furthermore, it is impossible to explain the polarization by using the Born terms alone and since the threshold energy ($E_{\gamma}^{\mathrm{lab}}=911$ MeV, $E_{\mathrm{total}}^{\mathrm{c.m.}}=1610$ MeV) is already higher than the rest masses of some baryon resonances, the presence of excited states in the direct and cross channels cannot be excluded. According to previous workers,[10] high spin resonances have little effect in improving the fit to the data. For this reason, and

TABLE II. Particles of interest and the low spin baryon resonances up to 1800 MeV.

Particle	J^{P}	Mass (MeV)	Width (MeV)
p	$\frac{1}{2}^{+}$	938.2796	
K^{+}	0^{-}	493.669	
K^{*+}	1^{-}	891.8	
Λ	$\frac{1}{2}^{+}$	1115.60	
Σ	$\frac{1}{2}^{+}$	1192.46	
N1 (1470)	$\frac{1}{2}^{+}$	1400 to 1480	120 to 350 (200)
N2 (1520)	$\frac{3}{2}^{-}$	1510 to 1530	100 to 140 (125)
N3 (1535)	$\frac{1}{2}^{-}$	1520 to 1560	100 to 250 (150)
N4 (1650)	$\frac{1}{2}^{-}$	1620 to 1680	100 to 200 (150)
N5 (1700)	$\frac{3}{2}^{-}$	1670 to 1730	70 to 120 (120)
N6 (1710)	$\frac{1}{2}^{+}$	1680 to 1740	100 to 140 (120)
N7 (1720)	$\frac{3}{2}^{+}$	1690 to 1800	150 to 250 (200)
Y1 (1405)	$\frac{1}{2}^{-}$	1405	30 to 50 (40)
Y2 (1670)	$\frac{1}{2}^{-}$	1660 to 1680	20 to 60 (40)
Y3 (1800)	$\frac{1}{2}^{-}$	1700 to 1850	200 to 400 (300)
Y4 (1660)	$\frac{1}{2}^{+}$	1580 to 1690	30 to 200 (100)
Y5 (1750)	$\frac{1}{2}^{-}$	1730 to 1820	50 to 160 (75)

the fact that the energies to be used in nuclear physics are close to threshold and hence high angular momentum states cannot be easily excited, we only include resonances up to spin $\frac{3}{2}$ in the s channel and spin $\frac{1}{2}$ in the u channel. The possible effect of resonances in the t channel or spin $\frac{3}{2}$ resonances in the u channel is left for future consideration. Table II shows all resonances[11] under consideration where we refer to the three low-lying Λ^* resonances as $Y1-Y3$ and the two low-lying Σ^* resonances as $Y4$ and $Y5$.

As noted earlier, in order to keep relativistic invariance one cannot use the standard method of partial-wave amplitudes. It is, however, possible to include resonant terms in a relativistic invariant way by using the same procedure used for the Born terms. Figures 1(f)—(h) show the Feynman diagrams for such terms. Because the diagrams for each of the baryon resonances are identical (apart from the coupling constants) only three diagrams are shown representing the spin $\frac{1}{2}$ and spin $\frac{3}{2}$ resonances in the s channel and the spin $\frac{1}{2}$ resonances in the u channel, respectively.

The propagators for the spin 0, $\frac{1}{2}$, and 1 states can be found in several sources, such as Refs. 7, 12, and 13. The spin $\frac{3}{2}$ propagator is derived by Pilkuhn[12] as well as by Schwinger.[13] A compilation of all propagators is given in Table III. It should be noted that the spin $\frac{3}{2}$ propagator given in these references is not unambiguously defined. In order to ensure gauge invariance it is necessary[14] that the mass appearing in the numerator of the spin $\frac{3}{2}$ propagator be replaced by the total invariant energy given by $\sqrt{s}$. Furthermore, it is necessary to replace M^2 by $M^2-iM\Gamma$ in the denominator of the propagators in order to take care of the finite width of the unstable particles.

The vertex factors for the Born terms (including the vector kaon exchange term) can be found in Refs. 5, 8, or 12. The spin $\frac{3}{2}$ vertex factors are constructed in analogy with those of the delta resonance of pion photoproduction,[3,4,12] apart from replacing the mass M_{N^*} by $\sqrt{s}$ as in the case of the propagator. For the spin $\frac{1}{2}$ nucleon resonance the vertex factors are similar to the vertex factors of the proton exchange term. In fact, the structure of the $K\Lambda N^*$ vertex is identical to the $K\Lambda p$ vertex. The only difference is at the $N^*\gamma p$ vertex, where the proton has to make a transition from its ground state to one of its excited states. This cannot be achieved by an electrostatic potential, but by electromagnetic currents only. Hence, the only possible coupling is through the magnetic moment. Therefore, the $p\gamma p$ coupling $e\not{\epsilon}+\mu_p\not{p}_\gamma\not{\epsilon}$ has to be replaced by $\mu_{N^*}\not{p}_\gamma\not{\epsilon}$ for the $N^*\gamma p$ vertex. This replacement is also necessary to ensure gauge invariance. The different parity states are accounted for by inserting the γ_5 matrix in the appropriate place. A collection of all vertex factors is given in Table IV. The two independent coupling constants of each spin $\frac{1}{2}$ resonance can be combined into one effective constant, and the three independent coupling constants of each spin $\frac{3}{2}$ state can be grouped into two effective parameters representing the two independent coupling modes as given below:

TABLE III. Propagators for particles with mass M, width Γ, and four-momentum q.

spin $\frac{1}{2}$	$\dfrac{\not{q}+M}{q^2-M^2+iM\Gamma}$
spin $\frac{3}{2}$	$\dfrac{\not{q}+\sqrt{s}}{3(q^2-M^2+iM\Gamma)}\left[g_{\mu\nu}+\gamma_\nu\gamma_\mu-\dfrac{2}{s}q_\mu q_\nu-\dfrac{1}{\sqrt{s}}(\gamma_\mu q_\nu-\gamma_\nu q_\mu)\right]$
spin 0	$\dfrac{1}{q^2-M^2}$
spin 1	$\dfrac{1}{q^2-M^2}\left[-g_{\mu\nu}+\dfrac{q_\mu q_\nu}{M^2}\right]$

TABLE IV. Vertex factors for the reaction $\gamma+p\to K^++\Lambda^0$. The mass M equals 1000 MeV, and is inserted to make $g_{K^*K\gamma}$ dimensionless. For the same reason $g_{K\Lambda N^*}$ is divided by M_{N^*}.

$p\gamma p$	$e\not{\epsilon}+\mu_p\not{p}_\gamma\not{\epsilon}$
ΛK^+p	$ig_{K\Lambda N}\gamma_5$
ΣK^+p	$ig_{K\Sigma N}\gamma_5$
$K^+\gamma K^+$	$e\epsilon\cdot(2p_K-p_\gamma)$
$\Lambda\gamma\Lambda$	$\mu_\Lambda\not{p}_\gamma\not{\epsilon}$
$\Sigma\gamma\Lambda$	$\mu_T\not{p}_\gamma\not{\epsilon}$
$K^{*+}\gamma K^+$	$\dfrac{g_{K^*K\gamma}}{M}\epsilon^{\mu\nu\rho\sigma}\epsilon_\nu(p_\gamma)_\rho(p_\Lambda-p_p)_\sigma$
$K^{*+}\Lambda p$	$g^V_{K^*\Lambda N}\gamma^\mu+\dfrac{g^T_{K^*\Lambda N}}{M_\Lambda+M_p}(\not{p}_\Lambda-\not{p}_p)\gamma^\mu$
$N^*(\frac{1}{2}^+)\gamma p$	$\mu_{N^*}\not{p}_\gamma\not{\epsilon}$
$N^*(\frac{1}{2}^+)K^+\Lambda$	$ig_{K\Lambda N^*}\gamma_5$
$N^*(\frac{1}{2}^-)\gamma p$	$i\mu_{N^*}\not{p}_\gamma\not{\epsilon}\gamma_5$
$N^*(\frac{1}{2}^-)K^+\Lambda$	$g_{K\Lambda N^*}$
$N^*(\frac{3}{2}^+)\gamma p$	$i\left[g^a_{N^*p\gamma}\left[\epsilon^\nu-\dfrac{\not{\epsilon}p^\nu_\gamma}{\sqrt{s}+M_p}\right]+g^b_{N^*p\gamma}\dfrac{\epsilon\cdot p_p p^\nu_\gamma-p_\gamma\cdot p_p\epsilon^\nu}{(\sqrt{s}+M_p)^2}\right]\gamma_5$
$N^*(\frac{3}{2}^+)K^+\Lambda$	$\dfrac{g_{K^+\Lambda N^*}}{M_{N^*}}p^\mu_\Lambda$
$N^*(\frac{3}{2}^-)\gamma p$	$\left[g^a_{N^*p\gamma}\left[\epsilon^\nu-\dfrac{\not{\epsilon}p^\nu_\gamma}{\sqrt{s}-M_p}\right]+g^b_{N^*p\gamma}\dfrac{\epsilon\cdot p_p p^\nu_\gamma-p_\gamma\cdot p_p\epsilon^\nu}{(\sqrt{s}-M_p)^2}\right]$
$N^*(\frac{3}{2}^-)K^+\Lambda$	$\dfrac{ig_{K^+\Lambda N^*}}{M_{N^*}}p^\mu_\Lambda\gamma_5$
$Y^*(\frac{1}{2}^+)\gamma\Lambda$	$\mu_{Y^*}\not{p}_\gamma\not{\epsilon}$
$Y^*(\frac{1}{2}^+)K^+p$	$ig_{KNY^*}\gamma_5$
$Y^*(\frac{1}{2}^-)\gamma\Lambda$	$i\mu_{Y^*}\not{p}_\gamma\not{\epsilon}\gamma_5$
$Y^*(\frac{1}{2}^-)K^+p$	g_{KNY^*}

$$G_{N1}=\kappa_{N1}g_{KAN1}\ ,$$
$$G_{N4}=\kappa_{N4}g_{KAN4}\ ,$$
$$G^1_{N5}=g^a_{N5\gamma p}g_{KAN5}\ ,$$
$$G^2_{N5}=g^b_{N5\gamma p}g_{KAN5}\ , \qquad (5)$$
$$G^1_{N7}=g^a_{N7\gamma p}g_{KAN7}\ ,$$
$$G^2_{N7}=g^b_{N7\gamma p}g_{KAN7}\ ,$$
$$G_{Y5}=\kappa_{Y5}g_{KNY5}\ .$$

By using the appropriate vertex factors and propagators the scattering amplitude can be calculated in the usual way. Table I shows the resulting invariant amplitudes.

III. MULTIPOLE DECOMPOSITION OF THE OPERATOR

As an aid in comparing our photoproduction operator to other approaches, and for possible future considerations of unitarity and time reversal invariance,[15–17] we present a multipole decomposition of our operator using the techniques and notation of Ref. 6. Initially, we write the matrix elements appearing in Eq. (1) in two-component form by expressing the γ matrices in terms of the Pauli σ matrices and writing the "small" component of the Dirac spinors in terms of σ matrices times the large component. In the K-Λ^0 center of momentum (c.m.) frame, the kinematic variables are defined as

$$p_p=(E_p,-\mathbf{k}),\ \ p_\gamma=(k,\mathbf{k})\ ,$$
$$p_K=(\omega,\mathbf{q}),\ \ p_\Lambda=(E_\Lambda,-\mathbf{q})\ .$$

The reaction angle $\cos\theta=\hat{\mathbf{k}}\cdot\hat{\mathbf{q}}=x$, where $\hat{\mathbf{k}}=\mathbf{k}/|\mathbf{k}|$ and $\hat{\mathbf{q}}=\mathbf{q}/|\mathbf{q}|$. The z axis is the quantization axis and the gauge (transverse) condition on the photon polarization is the usual $\epsilon_0=0$, $\boldsymbol{\epsilon}\cdot\mathbf{k}=0$.

In the c.m. frame, the matrix element M_{fi} of Eq. (1) can be written as,

$$\bar{u}(p_\Lambda)\sum_{i=1}^{4}A_i(s,t)M_iu(p_p)=\left[\frac{E_\Lambda+M_\Lambda}{2M_\Lambda}\right]^{1/2}\left[\frac{E_p+M_p}{2M_p}\right]^{1/2}\langle\chi(\Lambda)|\mathcal{F}|\chi(p)\rangle\ , \qquad (6)$$

where

$$\mathcal{F}=\boldsymbol{\sigma}\cdot\boldsymbol{\epsilon}\mathcal{F}_1+i(\boldsymbol{\sigma}\cdot\hat{\mathbf{q}})(\boldsymbol{\sigma}\cdot\hat{\mathbf{k}}\times\boldsymbol{\epsilon})\mathcal{F}_2+(\boldsymbol{\sigma}\cdot\hat{\mathbf{k}})(\hat{\mathbf{q}}\cdot\boldsymbol{\epsilon})\mathcal{F}_3+(\boldsymbol{\sigma}\cdot\hat{\mathbf{q}})(\hat{\mathbf{q}}\cdot\boldsymbol{\epsilon})\mathcal{F}_4 \qquad (7)$$

and the $\mathcal{F}_i$ are given in terms of the A_i in many references.[5,8]

The multipoles $E_{l\pm}$, $M_{l\pm}$ are defined by the following equation:

$$\widetilde{M}_l(s)=\int_{-1}^{1}dx\,D_l(x)\widetilde{\mathcal{F}}(s,t)\ , \qquad (8)$$

where

$$\widetilde{\mathcal{F}}(s,t)=\begin{bmatrix}\mathcal{F}_1\\ \mathcal{F}_2\\ \mathcal{F}_3\\ \mathcal{F}_4\end{bmatrix},\quad \widetilde{M}_l(s)=\begin{bmatrix}E_{l+}\\ E_{l-}\\ M_{l+}\\ M_{l-}\end{bmatrix},$$

and the matrices $D_l(x)$ are given in Ref. 6. The multipole amplitudes can now be calculated by direct integration of Eq. (8) which lead to Legendre functions of the second kind,

$$Q_l(y)=\tfrac{1}{2}\int_{-1}^{1}dx\frac{P_l(x)}{y-x}$$

and combinations of these functions given by

$$R_l(y)=\frac{l}{2l+1}Q_{l-1}(y)+\frac{l+1}{2l+1}Q_{l+1}(y)\ ,$$
$$T_l(y)=\frac{l}{2l+1}[Q_{l-1}(y)-Q_{l+1}(y)]\ .$$

These functions occur with arguments E_1–E_4 given by

$$E_1=-E_\Lambda/q,\ \ E_2=(M^2_\Lambda-M^2_\Sigma-2E_\Lambda k)/2kq\ ,$$
$$E_3=\omega/q,\ \ E_4=(2k\omega+M^2_{K^*}-M^2_k)/2kq\ .$$

Since it may be desirable to investigate the contributions of the Born terms and the resonance terms individually, we give the multipole amplitudes separately.

A. Born terms

For convenience the result is presented in matrix form,

$$\widetilde{M}_l^{\,\mathrm{Born}}=\sum_{i=1}^{4}\widetilde{Q}_l(E_i)\widetilde{H}_i+\widetilde{C}_l\ , \qquad (9)$$

where

$$\widetilde{Q}_l(E_i)=\frac{1}{2(l+1)}\begin{bmatrix} Q_l(E_i) & Q_{l+1}(E_i) & R_l(E_i) & R_{l+1}(E_i) & T_l(E_i) & T_{l+1}(E_i)\\ \frac{l+1}{l}Q_l(E_i) & \frac{l+1}{l}Q_{l-1}(E_i) & \frac{l+1}{l}R_l(E_i) & \frac{l+1}{l}R_{l-1}(E_i) & -\left[\frac{l+1}{l}\right]^2T_l(E_i) & -\left[\frac{l+1}{l-1}\right]T_{l-1}(E_i)\\ Q_l(E_i) & Q_{l+1}(E_i) & R_l(E_i) & R_{l+1}(E_i) & -\frac{1}{l}T_l(E_i) & 0\\ -\frac{(l+1)}{l}Q_l(E_i) & -\frac{(l+1)}{l}Q_{l-1}(E_i) & -\frac{(l+1)}{l}R_l(E_i) & -\frac{(l+1)}{l}R_{l-1}(E_i) & \frac{(l+1)}{l^2}T_l(E_i) & 0\end{bmatrix}.$$

The six and four element column vectors $\widetilde{H}_i$ and $\widetilde{C}_l$ depend only upon kinematic factors and coupling constants, and are given by

$$\tilde{H}_1=\frac{g_\Lambda e\kappa_\Lambda}{M_\Lambda}\begin{bmatrix}\frac{1}{q}(E_\Lambda-M_\Lambda a)\\ -\frac{M_\Lambda a}{E_\Lambda+M_\Lambda}\\ 1\\ -1\\ -a\\ \frac{-qa}{E_\Lambda+M_\Lambda}\end{bmatrix},\quad \tilde{H}_2=\frac{2G_\Sigma e}{M_\Lambda+M_\Sigma}\begin{bmatrix}\frac{1}{q}\left[E_\Lambda-\frac{M_\Sigma+M_\Lambda}{2}a\right]\\ \frac{1}{E_\Lambda+M_\Lambda}\left[\frac{M_\Sigma+M_\Lambda}{2}a-E_\Lambda(a-1)\right]\\ 1\\ -1\\ -a\\ \frac{qa}{E_\Lambda+M_\Lambda}\end{bmatrix},\quad \tilde{H}_3=\begin{bmatrix}0\\0\\0\\0\\ \frac{2g_\Lambda e}{E_p+M_p}\\ -\frac{2g_\Lambda eq}{k(E_\Lambda+M_\Lambda)}\end{bmatrix},$$

$$\tilde{H}_4=\frac{1}{M}\begin{bmatrix}\frac{1}{q}\{-G_V(2E_\Lambda+\omega+aM^+)+\frac{G_T}{M^+}[\omega M^- -a(M_K^2-2k\omega)]\}\\ \frac{1}{E_\Lambda+M_\Lambda}\{G_V[\omega(a-1)+aM^+]+\frac{G_T}{M^+}[(a-1)(2E_\Lambda-\omega)M^-+a(M_K^2-2k\omega)]\}\\ G_V+\frac{G_T}{M^+}(M^- -2ka)\\ \frac{q(a-1)}{E_\Lambda+M_\Lambda}\left[G_V+\frac{G_T}{M^+}(M^- -2a(E_p+M_p))\right]\\ -G_Va+\frac{G_T}{M^+}[2(a-1)(E_p+k)-M^-a]\\ -q\left\{\frac{G_V}{E_\Lambda+M_\Lambda}a+\frac{G_T}{M^+}\left[\frac{2(E_p+k)}{E_p+M_p}+\frac{M^-a}{E_\Lambda+M_\Lambda}\right]\right\}\end{bmatrix}, \tag{10}$$

$$\tilde{C}_l=g_\Lambda e\begin{bmatrix}\left[\frac{(\kappa_p+1)a}{2(E_p+k)}+\frac{\kappa_p}{2M_p}\right]\delta_{l,0}\\ 0\\ 0\\ \frac{q}{E_\Lambda+M_\Lambda}\left[\frac{a(\kappa_p+1)}{2(E_p+k)}-\frac{(a-1)\kappa_p}{M_p}\right]\delta_{l,1}\end{bmatrix},$$

where $M^{\pm}=M_\Lambda\pm M_p$ and $a=1+k/(E_p+M_p)$.

B. Resonance terms

The multipoles coming from the $\frac{1}{2}^+$ and $\frac{1}{2}^-$ resonances in the s channel have a simple form since their amplitudes $A_i^{1/2+}$ and $A_i^{1/2-}$ only depend upon s and not the reaction angle θ. Here $A_i^{1/2+}$ and $A_i^{1/2-}$ denote, respectively, the parts of the amplitudes A_i in Table I that have the coupling constants G_{N1} and G_{N4} as forefactors. The multipole amplitudes for the spin $\frac{1}{2}$ resonances are given by

$$\begin{aligned}E_{l+}^{1/2\pm}&=k[-aA_1^{1/2\pm}+(E_p+k)A_3^{1/2\pm}]\delta_{l,0}\,,\\ E_{l-}^{1/2\pm}&=0\,,\\ M_{l+}^{1/2\pm}&=0\,,\\ M_{l-}^{1/2\pm}&=\frac{kq}{E_\Lambda+M_\Lambda}[aA_1^{1/2\pm}-(a-1)(E_p+k)A_3^{1/2\pm}]\delta_{l,1}\,.\end{aligned} \tag{11}$$

The spin $\frac{3}{2}$ resonance amplitudes $A_i^{3/2+}$ and $A_i^{3/2-}$ depend on x and are rewritten in terms of new quantities B_1, B_3, D_1, and D_3, which are independent of x and are defined by

$$\begin{aligned}A_1^{3/2+}&=B_1^+-\frac{G_{N7}^1kqx}{(s-M_{N7}^2+iM_{N7}\Gamma_{N7})(M_p+\sqrt{s})M_{N7}}\\ &=B_1^+-D_1^+kqx\,,\\ A_3^{3/2+}&=B_3^+-\frac{G_{N7}^2kqx}{(s-M_{N7}^2+iM_{N7}\Gamma_{N7})(M_p+\sqrt{s})^2M_{N7}}\\ &=B_3^+-D_3^+kqx\,,\end{aligned} \tag{12}$$

$$A_1^{3/2-}=B_1^- - \frac{G_{N5}^1 kqx}{(s-M_{N5}^2+iM_{N5}\Gamma_{N5})(\sqrt{s}-M_p)M_{N5}}$$
$$=B_1^- - D_1^- kqx\ ,$$
$$A_3^{3/2-}=B_3^- - \frac{G_{N5}^2 kqx}{(s-M_{N5}^2+iM_{N5}\Gamma_{N5})(\sqrt{s}-M_p)^2 M_{N5}}$$
$$=B_3^- - D_3^- kqx\ .$$

Finally, the spin $\frac{3}{2}$ multipoles can be written as

$$E_{l+}^{3/2\pm}=\left[\left[I_1^\pm+\frac{I_4^\pm-I_6^\pm}{3}\right]\delta_{l,0}+\frac{(I_5^\pm+I_2^\pm)}{6}\delta_{l,1}\right],$$
$$E_{l-}^{3/2\pm}=-\tfrac{1}{6}(I_6^\pm+2I_4^\pm)\delta_{l,2}\ ,$$
$$M_{l+}^{3/2\pm}=\tfrac{1}{6}(I_5^\pm-I_2^\pm)\delta_{l,1}\ , \tag{13}$$
$$M_{l-}^{3/2\pm}=\left[\left[\frac{I_2^\pm-I_5^\pm}{3}+I_3^\pm\right]\delta_{l,1}+\tfrac{1}{6}I_6^\pm\delta_{l,2}\right],$$

where the quantities $I_1^\pm,\ldots,I_6^\pm$ contain all the kinematic factors and coupling constants and are given by

$$I_1^\pm=k[(E_p+k)B_3^\pm-aB_1^\pm+E_\Lambda A_4^{3/2\pm}]\ ,$$
$$I_2^\pm=kq[2(a-1)(E_p+k)A_2^{3/2\pm}-aA_4^{3/2\pm}]\ ,$$
$$I_3^\pm=\frac{kq}{E_\Lambda+M_\Lambda}[aB_1^\pm-(a-1)(E_p+k)B_3^\pm -(a-1)E_\Lambda A_4^{3/2\pm}]\ , \tag{14}$$
$$I_4^\pm=-\frac{kq^2}{E_\Lambda+M_\Lambda}[2(E_p+k)A_2^{3/2\pm}+aA_4^{3/2\pm}]\ ,$$
$$I_5^\pm=kq[A_4^\pm+kaD_1^\pm+k(E_p+k)D_3^\pm]\ ,$$
$$I_6^\pm=\frac{-k^2q^2}{E_\Lambda+M_\Lambda}\left[\frac{1}{E_p+M_p}A_4^{3/2\pm}+aD_1^\pm -(a-1)(E_p+k)D_3^\pm\right].$$

The multipoles coming from the spin $\frac{1}{2}^-$ resonances in the u channel can be expressed by using the matrix $\widetilde{Q}_l(E)$, defined in Eq. (9):

$$\widetilde{M}_l^{Y^*}=\widetilde{Q}_l(E_5)\widetilde{H}_5\ ,$$

where

$$E_5=\frac{M_\Lambda^2-M_{Y5}^2-2E_\Lambda k+iM_{Y5}\Gamma_{Y5}}{2kq}$$

and

$$\widetilde{H}_5=\frac{2G_{Y5}ekq}{M_{Y5}+M_\Lambda}\begin{bmatrix} \dfrac{1}{q}\left[\dfrac{a}{2}\left[M_{Y5}-M_\Lambda-\dfrac{i}{2}\Gamma_{Y5}\right]-E_\Lambda\right] \\ \dfrac{1}{E_\Lambda+M_\Lambda}\left[\dfrac{a}{2}\left[M_{Y5}-M_\Lambda-\dfrac{i}{2}\Gamma_{Y5}\right]-\dfrac{kE_\Lambda}{E_p+M_p}\right] \\ -1 \\ -\dfrac{qk}{(E_p+M_p)(E_\Lambda+M_\Lambda)} \\ a \\ \dfrac{qa}{E_\Lambda+M_\Lambda} \end{bmatrix}. \tag{15}$$

IV. NONRELATIVISTIC OPERATOR

For kaon production from nuclei where the initial and final (hyperon) single particle states are described by conventional (Schrödinger) wave functions, we require a production operator which operates on two-component wave functions. We obtain such an operator by reducing the free Dirac spinors for the lambda and the proton to their two-component form. If we then evaluate the matrix element in Eq. (1) in a general frame, we can identify those contributions coming from the big-big, big-small, small-big, and small-small parts of the Dirac spinors. Carrying this out we can write the matrix element in Eq. (1) as

$$\bar{u}(l)\sum_{i=1}^{4}M_iA_i(s,t)u(p)=\left[\frac{E_p+M_p}{2M_p}\right]^{1/2}\left[\frac{E_\Lambda+M_\Lambda}{2M_\Lambda}\right]^{1/2}$$
$$\times\langle\chi(\Lambda)|F_1(\boldsymbol{\sigma}\cdot\boldsymbol{\epsilon})+F_2(\boldsymbol{\sigma}\cdot\mathbf{k})(\boldsymbol{\epsilon}\cdot\mathbf{p})+F_3(\boldsymbol{\sigma}\cdot\mathbf{k})(\boldsymbol{\epsilon}\cdot\mathbf{l})+F_4(\boldsymbol{\sigma}\cdot\mathbf{p})(\boldsymbol{\epsilon}\cdot\mathbf{p})+F_5(\boldsymbol{\sigma}\cdot\mathbf{p})(\boldsymbol{\epsilon}\cdot\mathbf{l})$$
$$+F_6(\boldsymbol{\sigma}\cdot\mathbf{l})(\boldsymbol{\epsilon}\cdot\mathbf{p})+F_7(\boldsymbol{\sigma}\cdot\mathbf{l})(\boldsymbol{\epsilon}\cdot\mathbf{l})+F_8(\boldsymbol{\sigma}\cdot\boldsymbol{\epsilon})(\boldsymbol{\sigma}\cdot\mathbf{k})(\boldsymbol{\sigma}\cdot\mathbf{p})+F_9(\boldsymbol{\sigma}\cdot\mathbf{l})(\boldsymbol{\sigma}\cdot\mathbf{k})(\boldsymbol{\sigma}\cdot\boldsymbol{\epsilon})$$
$$+F_{10}(\boldsymbol{\sigma}\cdot\mathbf{l})(\boldsymbol{\sigma}\cdot\boldsymbol{\epsilon})(\boldsymbol{\sigma}\cdot\mathbf{p})+F_{11}(\boldsymbol{\sigma}\cdot\mathbf{l})(\boldsymbol{\sigma}\cdot\mathbf{k})(\boldsymbol{\epsilon}\cdot\mathbf{p})(\boldsymbol{\sigma}\cdot\mathbf{p})+F_{12}(\boldsymbol{\sigma}\cdot\mathbf{l})(\boldsymbol{\sigma}\cdot\mathbf{k})(\boldsymbol{\epsilon}\cdot\mathbf{l})(\boldsymbol{\sigma}\cdot\mathbf{p})|\chi(\mathrm{p})\rangle\ , \tag{16}$$

where $p=p_{\rm p}$ and $l=p_\Lambda$ and the F_i are given in terms of the A_i of Table I by

$$F_1=-kA_1+k\cdot pA_3+k\cdot lA_4 \;,$$
$$F_2=A_3 \;,$$
$$F_3=A_4 \;,$$
$$F_4=-(2A_2k\cdot l+kA_3)/(E_{\rm p}+M_{\rm p}) \;,$$
$$F_5=(2A_2k\cdot p-kA_4)/(E_{\rm p}+M_{\rm p}) \;,$$
$$F_6=(2A_2k\cdot l-kA_3)/(E_\Lambda+M_\Lambda) \;,$$
$$F_7=-(2A_2k\cdot p+kA_4)/(E_\Lambda+M_\Lambda) \;,$$
$$F_8=A_1\,/(E_{\rm p}+M_{\rm p}) \;,$$
$$F_9=A_1\,/(E_\Lambda+M_\Lambda) \;,$$
$$F_{10}=(kA_1+k\cdot pA_3+k\cdot lA_4)/[(E_{\rm p}+M_{\rm p})(E_\Lambda+M_\Lambda)] \;,$$
$$F_{11}=A_3\,/[(E_{\rm p}+M_{\rm p})(E_\Lambda+M_\Lambda)] \;,$$
$$F_{12}=A_4\,/[(E_{\rm p}+M_{\rm p})(E_\Lambda+M_\Lambda)] \;.$$

The terms in Eq. (16) containing F_1—F_3 come from products of the big parts of the Dirac spinors, while the terms F_{10}—F_{12} come from products of the small parts of the Dirac spinors. Since the nonrelativistic wave functions of the proton and the lambda in the nucleus already implicitly contain some portion of the small component of the Dirac spinors, we should certainly discard terms containing F_{10}—F_{12}. A more extreme nonrelativistic limit would be to further discard terms involving F_4—F_9 since they involve a small component from either the lambda or the proton. Previous workers[1,2] have kept the complete $\sigma\cdot\epsilon$ term but have assumed frozen protons and have examined (apart from the second paper in Ref. 1) kaon production at 0°. Under these conditions only terms F_1 and F_9 contribute, and the F_9 term plays a significant role.

In pion photoproduction near threshold it is well known that the leading Kroll-Ruderman term (equivalent to the F_1 term) provides a good description of the production process. However, in the case of kaon photoproduction, the much larger change in rest mass during the production process requires much more energetic photons and consequently much higher momenta and energies. It is not at all obvious that first-order relativistic corrections can be neglected. To investigate this point we compare the cross section calculated with only F_1, with F_1—F_9, and with F_1—F_{12} for different kinematics which might arise inside the nucleus. We choose the target proton to have momentum $|\mathbf{p}|$ and to be moving in various directions defined with respect to a laboratory coordinate system defined by choosing the z axis to be along the incident photon direction and the outgoing kaon to lie in the x-z plane. Given the initial proton momentum $\mathbf{p}$, the photon energy k, and the kaon laboratory angle θ, all remaining kinematic variables are defined.

As an example of our findings we show in Fig. 2 the cross section as a function of laboratory photon energy calculated with the F_1 term only, the F_1—F_9 terms, and with all the terms, F_1—F_{12} for 0° kaon production. The laboratory momenta of the proton for the three cases in

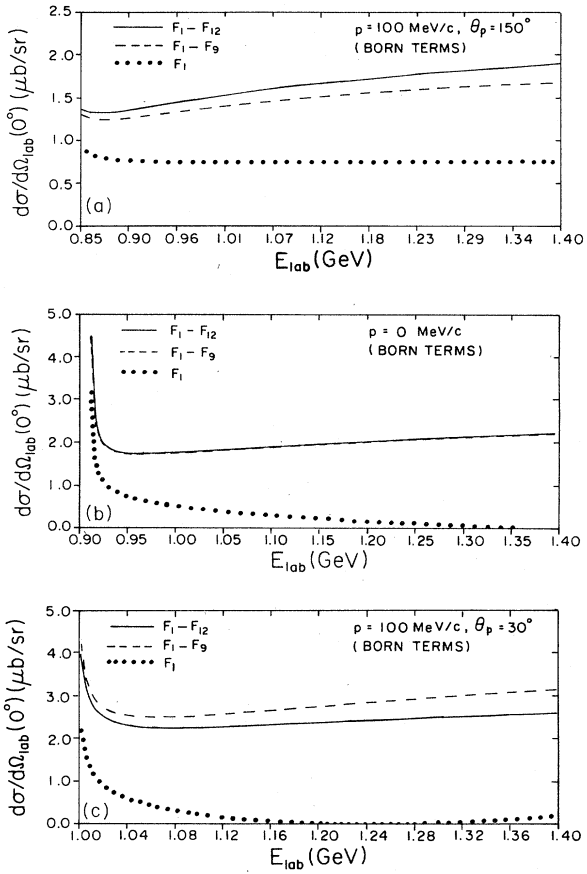

FIG. 2. The laboratory cross section as a function of photon energy for protons of three different momenta for kaons at 0° for the full operator and for two different nonrelativistic approximations: (a) $p_{\rm p}=100$ MeV/c, $\theta_{\rm p}=150°$; (b) $p_{\rm p}=0$; (c) $p_{\rm p}=100$ MeV/c, $\theta_{\rm p}=30°$.

Fig. 2 are $p_{\rm p}=100$ MeV/c for $\theta_{\rm p}=30°$ and 150°, and $p_{\rm p}=0$. When the photon energy is 1200 MeV, the magnitude of the recoiling lambda momenta for these three cases is 523, 248, and 375 MeV/c, respectively. One sees that the extreme nonrelativistic approximation (F_1 only) is a very bad approximation to the full calculation. On the other hand, for photon energies up to about 1400 MeV, the nonrelativistic approximation which only discards the terms of order p^2/M^2 in the production operator (F_{10}—F_{12}) is quite a good approximation. These three cases shown display a general result we found. Whether or not the F_1 term alone approximates the full operator is strongly dependent on kinematics.

To see if the errors made in using the F_1 term only tend to average out when integrating over the momentum distribution of both protons and lambdas in a nucleus, we performed a calculation of 0° kaon production from an infinitely massive pseudonucleus. We assume the initial and final "nucleus" has the same energy apart from the difference in rest mass of the proton and lambda. Therefore, the energy of the kaon, $\omega=k+M_{\rm p}-M_\Lambda$, and momentum of the kaon is $q=\sqrt{\omega^2-M_k^2}$ where k is the laboratory

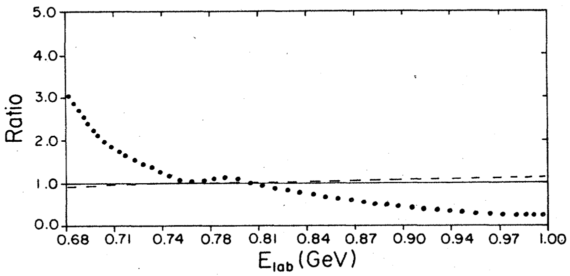

FIG. 3. The ratios $R_1=\sigma(F_1)/\sigma(F_1-F_{12})$ and $R_2=\sigma(F_1-F_9)/\sigma(F_1-F_{12})$ shown by $\cdots$ and — — —, respectively, are compared to one for laboratory energies from 0.680 to 1.0 GeV.

photon energy. In the kaon production amplitude the proton is taken to be on its mass shell, while the lambda energy $E_\Lambda=k+E_p-\omega$ and the lambda momentum $\mathbf{l}=\mathbf{k}+\mathbf{p}-\mathbf{q}$ and, therefore, the lambda is off its mass shell. With these kinematics we averaged the cross section over proton momenta p and angles θ_p by using a Fermi distribution,

$$\rho_p(p)=\frac{1}{1+\exp\left[\dfrac{p-p_0}{\Delta p}\right]}$$

with $p_0=100$ MeV/c and $\Delta p=50$ MeV/c which gives a rms value of the proton momentum equal to 200 MeV/c. For each value of $\mathbf{p}$ (for 0° kaon we have azimuthal symmetry), we weighted the cross section with a similar Fermi distribution for the lambda momentum $|\mathbf{l}|$. That is, lambda momenta which were too large to be kept in a nucleus were effectively discarded. We formed the ratios of cross sections $R_1=\sigma(F_1\text{ only})/\sigma(F_1-F_{12})$ and $R_2=\sigma(F_1-F_9)/\sigma(F_1-F_{12})$, and show the values of these ratios from threshold ($\approx$680 MeV) up to 1000 MeV in Fig. 3. Clearly keeping only the F_1 term is not justified, particularly at higher energies, while once again keeping the F_1-F_9 terms in a good approximation to the full operator.

We realize this procedure is only a rough description of kaon photoproduction from a nucleus where the production amplitude must be sandwiched between proton and lambda momentum space wave functions. However, our results suggest that the $\boldsymbol{\sigma}\cdot\boldsymbol{\epsilon}$ term with only the coefficient F_1 should not be used to include nuclear Fermi motion.

V. RESULTS AND CONCLUSION

Since our primary goal is to provide a kaon photoproduction operator suitable for use in nuclear physics where the final Λ^0 remains in the nucleus, we only consider production data from threshold ($E_\gamma^{\text{lab}}=911$ MeV) up to a laboratory photon energy of 1400 MeV. Higher energy photons result in larger momentum transfers to the nucleus

TABLE V. Coupling constants obtained by a least squares fit.

$g_\Lambda/\sqrt{4\pi}$	2.04	1.03	1.29
$G_\Sigma/\sqrt{4\pi}$	−1.24	−0.807	−3.85
$G_V/4\pi$	0.247	0.220	0.298
$G_T/4\pi$	−0.189	−0.048	−0.134
$G_{N1}/\sqrt{4\pi}$	0.0	1.47	1.80
$G_{N4}/\sqrt{4\pi}$	0.0	0.111	0.120
$G_{Y5}/\sqrt{4\pi}$	0.0	0.0	2.20
$G_{N7}^1/4\pi$	0.0	0.0	−0.051
$G_{N7}^2/4\pi$	0.0	0.0	−0.349
χ^2	6.10	2.98	2.30

for non 0° kaons and decrease the cross section appreciably.

Performing a least squares fit to the available data under 1400 MeV laboratory photo energy shows the insignificance of all resonances below threshold except the N1 (1470) resonance. The reason is probably that this resonance has the same spin-parity structure as the proton and interferes strongly with the dominant direct term. On the other hand, the most important resonance is the N4 (1650) state which is a $\frac{1}{2}^-$ state. This can be explained by the proximity of this resonance to threshold (only 40 MeV above threshold).

The next two resonances of importance are the spin $\frac{1}{2}^-$ state Y5 (1750) and the spin $\frac{3}{2}^+$ state N7 (1720). If one neglects resonances in the u channel, the χ^2 can be improved by including the spin $\frac{3}{2}^-$ state N5 (1700). We have neglected N5 (1700) in our calculations but we do present the amplitudes and multipole decomposition for this spin state. The remaining resonance states given in Table II provide little improvement in the reduced chi-square (chi-square per degree of freedom). We, therefore, restrict our considerations to the Born terms and the resonances N1 (1470), N4 (1650), Y5 (1750), and N7 (1720).

As a check on our procedure and computer programs,

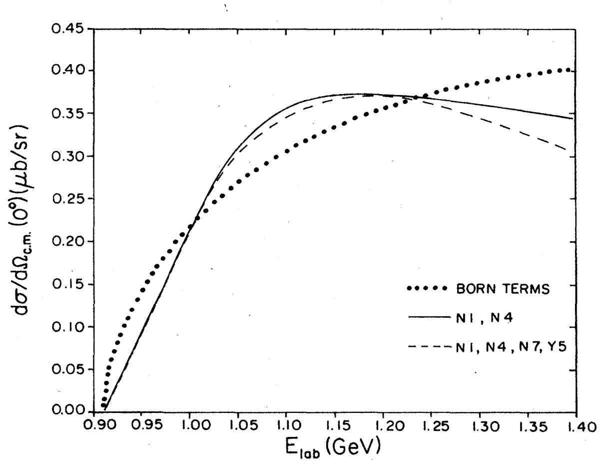

FIG. 4. Comparison of the theoretical c.m. cross section of the different models up to 1.4 GeV.

TABLE VI. Differential cross section data for the reaction $\gamma+p\rightarrow K^{+}+\Lambda^{0}$.

$\theta_K^{c.m.}$ (deg)	$\frac{d\sigma}{d\Omega}$ (10^{-30} cm^2/sr)	E_γ (MeV)	Ref.	$\theta_K^{c.m.}$ (deg)	$\frac{d\sigma}{d\Omega}$ (10^{-30} cm^2/sr)	E_γ (MeV)	Ref.
90.0	0.055±0.012	934	21	89.0	0.135±0.012	1172	25
60.0	0.067±0.006	942	5	69.5	0.196±0.012	1175	25
54.0	0.093±0.006	964	5	92.6	0.129±0.010	1190	18
31.1	0.134±0.008	976	21	15.0	0.379±0.027	1200	22
64.0	0.133±0.008	974	21	25.0	0.334±0.015	1200	22
56.5	0.112±0.012	994	25	30.0	0.341±0.019	1200	22
30.0	0.204±0.007	1002	21	30.0	0.353±0.019	1200	19
60.3	0.169±0.009	1003	21	35.0	0.300±0.014	1200	22
88.6	0.154±0.009	1004	21	42.0	0.284±0.015	1200	22
132.00	0.121±0.010	1004	21	49.0	0.282±0.016	1200	22
54.0	0.141±0.013	1005	25	55.0	0.276±0.016	1200	22
30.3	0.228±0.011	1013	21	63.0	0.241±0.016	1200	22
43.6	0.196±0.011	1020	21	70.0	0.202±0.014	1200	22
55.6	0.200±0.010	1018	21	78.0	0.194±0.017	1200	22
69.8	0.155±0.008	1022	21	85.0	0.154±0.018	1200	22
94.2	0.145±0.011	1024	21	90.0	0.152±0.012	1200	5
97.0	0.133±0.006	1018	21	90.2	0.143±0.007	1200	5
27.5	0.281±0.014	1040	21	92.1	0.143±0.010	1200	18
45.0	0.230±0.008	1036	21	127.0	0.134±0.040	1200	22
50.5	0.237±0.015	1047	25	91.7	0.124±0.009	1210	18
78.0	0.172±0.011	1047	25	89.7	0.125±0.007	1290	18
24.0	0.342±0.030	1050	19	6.0	0.321±0.033	1300	20
30.0	0.276±0.015	1054	21	10.0	0.314±0.020	1300	20
31.0	0.284±0.022	1054	22	15.0	0.316±0.016	1300	20
42.5	0.271±0.013	1055	21	20.0	0.328±0.013	1300	20
48.0	0.233±0.019	1054	22	30.0	0.337±0.018	1300	20
53.5	0.244±0.014	1054	21	40.0	0.330±0.020	1300	20
80.2	0.196±0.012	1051	21	50.0	0.295±0.015	1300	20
89.7	0.157±0.009	1054	21	60.0	0.233±0.015	1300	20
132.3	0.123±0.011	1060	21	70.0	0.200±0.017	1300	20
49.0	0.259±0.017	1064	25	80.0	0.176±0.018	1300	20
76.0	0.187±0.009	1064	25	89.8	0.143±0.009	1300	5
46.5	0.244±0.012	1080	21	90.0	0.137±0.017	1300	20
46.5	0.279±0.018	1080	22	89.4	0.129±0.007	1313	18
90.0	0.158±0.008	1080	21	62.0	0.239±0.020	1327	20
119.7	0.125±0.008	1080	21	52.7	0.270±0.022	1332	20
48.0	0.248±0.012	1090	25	89.1	0.142±0.007	1335	18
73.5	0.209±0.010	1090	25	43.2	0.299±0.020	1336	20
96.0	0.132±0.008	1090	25	33.5	0.340±0.019	1340	20
28.0	0.396±0.020	1100	19	23.3	0.361±0.015	1342	20
89.9	0.139±0.009	1100	5	17.7	0.349±0.018	1343	20
72.5	0.204±0.013	1110	25	11.2	0.334±0.025	1344	20
93.5	0.141±0.008	1110	25	88.9	0.136±0.007	1353	18
47.5	0.234±0.012	1113	25	88.7	0.123±0.008	1371	18
90.0	0.142±0.013	1130	21	88.6	0.116±0.007	1387	18
46.5	0.253±0.009	1150	25	17.5	0.279±0.024	1400	5
71.0	0.209±0.011	1150	25	25.0	0.271±0.021	1400	5
91.0	0.131±0.014	1150	25	32.5	0.294±0.021	1400	5
36.0	0.259±0.017	1160	5	40.0	0.261±0.014	1400	5
60.0	0.206±0.012	1160	5	45.0	0.266±0.016	1400	5
75.0	0.205±0.016	1160	5	60.0	0.232±0.011	1400	5
90.0	0.144±0.010	1160	5	75.0	0.181±0.013	1400	5
135.0	0.079±0.009	1160	5	90.0	0.157±0.008	1400	5
46.0	0.247±0.015	1170	25	142.5	0.117±0.010	1400	5

we reproduced Thom's results by fitting the Born terms to the data given in Ref. 5. Furthermore, we used the Born terms to fit all the cross section and polarization data given in Tables VI and VII. The resulting coupling constants, given in the first column of Table V, are in reasonable agreement with Thom's original parameters,[5] but the

TABLE VII. Polarization data where the polarization vector has been defined in the direction $\hat{p}_\gamma \times \hat{p}_K$.

$\theta_K^{c.m.}$ (deg)	$P(\hat{p}_\gamma \times \hat{p}_K)$	E_γ (MeV)	Ref.	$\theta_K^{c.m.}$ (deg)	$P(\hat{p}_\gamma \times \hat{p}_K)$	E_γ (MeV)	Ref.
93.0	−0.12±0.14	960	25	91.0	−0.09±0.11	1095	23
91.0	−0.19±0.14	963	24	47.6	−0.38±0.12	1100	10
93.0	−0.23±0.11	1000	23	72.8	−0.48±0.10	1100	10
94.0	−0.21±0.16	1015	25	90.0	−0.34±0.09	1100	5
92.0	−0.30±0.13	1018	24	94.4	−0.32±0.19	1100	10
61.0	−0.16±0.12	1020	24	90.0	−0.37±0.11	1121	23
87.0	−0.21±0.10	1026	23	46.0	−0.54±0.09	1160	10
86.0	−0.47±0.18	1040	25	70.0	−0.44±0.10	1160	10
85.0	−0.39±0.15	1050	24	90.0	−0.27±0.14	1160	10
49.8	−0.28±0.12	1054	10	90.0	−0.30±0.07	1200	5
76.8	−0.07±0.13	1054	10	90.0	−0.08±0.07	1300	5
80.0	−0.38±0.09	1056	23				

χ^2 per point for this fit is rather large.

Since we expect the fit to the polarization data to be more sensitive to the various resonances than the fit to the cross section data, we emphasized the polarization data by weighting them with a factor of 4 with respect to the cross section data. Although this leads to a small improvement in the χ^2 per point, the effect on the coupling constants is minor. Our final coupling constants given in Table V were obtained without any weighting.

In the second and third column of Table V we give the coupling constants and χ^2 values for the inclusion of the resonances N1 (1470) and N4 (1650) plus the resonances Y5 (1750) and N7 (1720), respectively. Clearly the addition of only N1 and N4 (model 1) improves the fit greatly ($\chi^2=2.98$) as compared to the Born terms alone which result in $\chi^2=6.10$. The further addition of Y5 and N7 (model 2) does improve the fit ($\chi^2=2.30$), but also results in a considerably more complicated operator.

Figure 4 illustrates the difference between the two models at a laboratory angle of 0° and shows the standard Born terms for comparison. It can be seen that the model with the Born terms only generally overpredicts the cross section at high energies as well as close to threshold, while the two models employing the resonances agree almost exactly up to an energy of about 1 GeV laboratory photon energy. In Fig. 5, the high energy behavior is shown. One can see that the resonant terms tend to decrease the effect of the nonresonant background at high energies. In Fig. 6, we compare the different models with data at a fixed laboratory photon energy of 1200 MeV. Here the two models agree pretty well, and there is no compelling reason to prefer one to the other. For this reason we show in Fig. 7 the polarization at 15° predicted by the two models. Here the difference is rather remarkable. More polarization data would be helpful in deciding whether or not more resonances should be included (model 2).

In conclusion, we find that the Born terms plus the addition of two spin $\frac{1}{2}$ resonances N1 (1470) and N4 (1650) in the direct channel (model 1) provide quite a good description of the available cross section and polarization data for the reaction $p(\gamma,K^+)\Lambda^0$ for laboratory energies from threshold ($E_\gamma^{lab}=911$ MeV) up to 1400 MeV. The inclusion of the resonances Y5 (1750) and N7 (1720) provides a somewhat better description of the data, but also adds increased complexity to the kaon photoproduction operator. Additional polarization data would be useful in

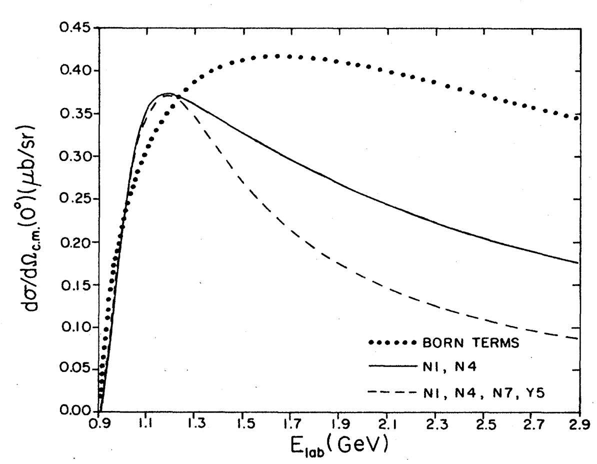

FIG. 5. Comparison of the theoretical c.m. cross section of the different models up to 2.9 GeV.

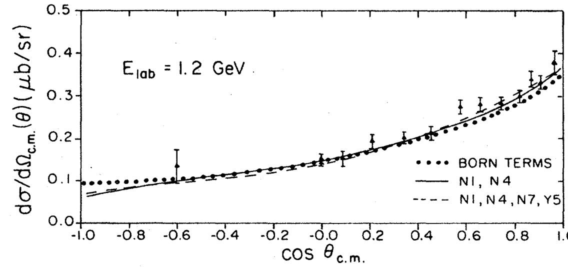

FIG. 6. Comparison of the theoretical c.m. cross section with data at 1.2 GeV.

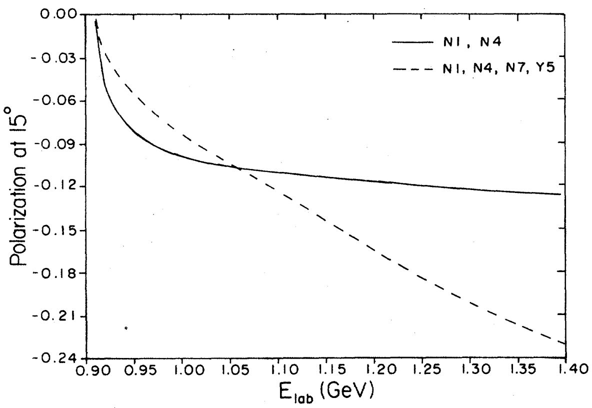

FIG. 7. Comparison of the polarization at 15° predicted by the various models. The polarization vector has been defined in the direction $\hat{p}_\gamma \times \hat{p}_K$.

determining the resonance contributions.

In Sec. III we gave the multipole decomposition of our operator for the convenience of other workers, and in Sec. IV we examined various nonrelativistic reductions of the operator. We find that the use of the $\boldsymbol{\sigma}\cdot\boldsymbol{\epsilon}$ term with F_1 alone is not justified, but do find that a less extreme nonrelativistic reduction of the operator works quite well near threshold. Finally, we suggest that it may be necessary to consider a relativistic treatment of the proton and lambda wave functions.

ACKNOWLEDGMENTS

We thank D. S. Onley for useful conversations and N. Mukhopadhyay for clarifying a puzzling point regarding the multipole decomposition. This work was supported in part by the U.S. Department of Energy Contract DE-AC02-79ER10397-3.

[1]Shian S. Hsiao and Stephen R. Cotanch, Phys. Rev. C **28**, 1668 (1983); in *Intersections between Particle and Nuclear Physics—1984 (Steamboat Springs),* Proceedings of the Conference on the Intersections of Particles and Nuclear Physics, AIP Conf. Proc. No. 123, edited by Richard E. Mischke (AIP, New York, 1984), p. 778.

[2]A. M. Bernstein, T. W. Donnelly, and G. N. Epstein, Nucl. Phys. **A358**, 195 (1981).

[3]I. Blomqvist and J. M. Laget, Nucl. Phys. **A280**, 405 (1977).

[4]S. Mehrotra and L. E. Wright, Nucl. Phys. **A362**, 461 (1981). See also S. Mehrotra, Ph.D. dissertation, Ohio University, 1981.

[5]H. Thom, Phys. Rev. **151**, 1322 (1966).

[6]F. A. Berends, A. Donnachie, and D. L. Weavers, Nucl. Phys. **B4**, 1 (1967).

[7]J. D. Bjorken and S. D. Drell, *Relativistic Quantum Mechanics* (McGraw-Hill, New York, 1964).

[8]M. Gourdin and J. Dufour, Nuovo Cimento **27**, 1410 (1963).

[9]L. Schachinger *et al.,* Phys. Rev. Lett. **41**, 1348 (1978).

[10]T. Fuji *et al.,* Phys. Rev. D **2**, 439 (1970). Y. Renard, Nucl. Phys. **B40**, 499 (1972).

[11]Particle Data Group, Rev. Mod. Phys. **56**, S1 (1984).

[12]H. Pilkuhn, *The Interactions of Hadrons* (North-Holland, Amsterdam, 1967).

[13]J. Schwinger, *Particles, Sources and Fields* (Addison-Wesley, Reading, Mass., 1970).

[14]R. A. Adelseck, M. S. thesis, Ohio University, 1985 (unpublished).

[15]L. Donald Pearlstein and Abraham Klein, Phys. Rev. **107**, 836 (1957).

[16]Kenneth M. Watson, Phys. Rev. **95**, 228 (1954).

[17]R. Wittmann, R. Davidson, and Nimai C. Mukhopadhyay, Phys. Lett. **142B**, 336 (1984).

[18]H. Göing, W. Schorsch, J. Tietze, and W. Weilnböck, Nucl. Phys. **B26**, 121 (1971).

[19]P. Feller *et al.,* Nucl. Phys. **B39**, 413 (1972).

[20]A. Bleckmann *et al.,* Z. Phys. **239**, 1 (1970).

[21]R. L. Anderson *et al.,* Phys. Rev. Lett. **9**, 131 (1962).

[22]C. W. Peck, Phys. Rev. **135**, B830 (1964).

[23]H. Thom, Phys. Rev. Lett. **11**, 433 (1963).

[24]M. Grilli, L. Mezzetti, M. Nigro, and E. Schiavuta, Nuovo Cimento **38**, 1467 (1965).

[25]B. Borgia *et al.,* Nuovo Cimento **32**, 218 (1964).